A molecular switch for initiating cell differentiation in Arabidopsis

Maite Sanmartín[1], Michael Sauer[1,4], Alfonso Muñoz[1,4], Jan Zouhar[1,4], Angel Ordóñez[1], Wilhelmina T. G. van de Ven[1,2], Elena Caro[3], María de la Paz Sánchez[3], Natasha V. Raikhel[2], Crisanto Gutiérrez[3], José J. Sánchez-Serrano[1] and Enrique Rojo[1,*]

[1] Centro Nacional de Biotecnología-CSIC, Cantoblanco, E-28049 Madrid, Spain, [2] Center for Plant Cell Biology and Department of Botany and Plant Sciences, University of California, Riverside, California 92521, USA,[3] Centro de Biología Molecular Severo Ochoa, CSIC-UAM, Cantoblanco, E-28049 Madrid, Spain.

[4] These authors have contributed equally to this work.

Corresponding Author: Dr. Enrique Rojo, PhD.

erojo@cnb.csic.es

Running title: MINIYO triggers cell differentiation

Keywords: differentiation, meristem, transcription, RNA polymerase II

Summary

Background: The onset of differentiation entails modifying the gene expression state of cells, to allow activation of developmental programs that are maintained repressed in the undifferentiated precursor cells [1, 2]. This requires a mechanism to change gene expression on a genome-scale. Recent evidence suggests that in mammalian stem cells derepression of developmental regulators during differentiation involves a shift from stalled to productive elongation of their transcripts [3-5], but factors mediating this shift have not been identified and the evidence remains correlative.

Results: We report the identification of the *MINIYO* (*IYO*) gene, a positive regulator of transcriptional elongation that is essential for cells to initiate differentiation in Arabidopsis. IYO interacts with RNA polymerase II and the Elongator complex and is required to sustain global levels of transcriptional elongation activity, specifically in differentiating tissues. Accordingly, *IYO* is expressed in embryos, meristems and organ primordia and not in mature tissues. Moreover, differential subcellular protein distribution further refines the domain of IYO function by directing nuclear accumulation, and thus its transcriptional activity, to cells initiating differentiation. Importantly, IYO over expression induces premature cell differentiation and leads to meristem termination phenotypes.

Conclusions: These findings identify IYO as a necessary and sufficient factor for initiating differentiation in Arabidopsis and suggest that the targeted nuclear accumulation of IYO functions as a transcriptional switch for this fate transition.

Highlights

MINIYO is necessary for initiating all events of cell differentiation in Arabidopsis

MINIYO sustains global levels of transcriptional elongation in differentiating tissues

Nuclear accumulation of MINIYO is directed to transition cells

MINIYO accumulation is sufficient to initiate cell differentiation

Introduction

Cell differentiation entails two sequential decisions by precursor cells. The first one, shared by every event of differentiation, is whether to self-renew or initiate this fate transition. The second decision, specific for each differentiation process, is what cell fate to attain. Genetic networks determining progression into specific fates have been described in both animals and plants [6]. In contrast, very little is known about the mechanisms that trigger differentiation in the first place, possibly because this step is essential for organism viability and thus less amenable to genetic analysis. In plants, differentiation occurs in defined niches called meristems and is easily traceable due to the immobility of cells. In addition, plants have high developmental plasticity and tolerate drastic changes in their body plan. This renders them a powerful model system to search for genetic factors that determine the timing of cell differentiation.

It has been proposed that plant hormone gradients serve as instructive signals to set the boundaries where cell differentiation starts in meristems. For instance, crosstalk between auxins and cytokinins delimits the transition zone in root meristems [7] and auxin accumulation defines the position of future organ primordia in the shoot meristem [8]. Several genes involved in generating, perceiving and transducing these hormonal signals have been linked to these developmental responses [9]. However, it is unknown how the decision to initiate differentiation is taken at the cellular level. Differentiation implies a global transcriptional reprogramming, so those factors likely target the transcriptional condition of the cell. In metazoans it is thought that the undifferentiated status is the default transcriptional state maintained by self-reinforcement of networks that direct renewal and

repression of genes directing differentiation [2, 10]. Remarkably, in mammalian stem cells (SCs) chromatin is in an open state [10, 11], implying that the transcriptional machinery has access to the promoters of genes directing differentiation even though they remain transcriptionally inactive. In support of this hypothesis, there is genome-wide transcriptional initiation but productive elongation of developmental regulators directing differentiation is prevented [3-5]. Differentiation in mammalian SCs may thus involve the active removal of hindrances preventing transcriptional elongation of developmental genes or, alternatively, the accumulation of a necessary factor for elongation in the progeny destined for differentiation. Interestingly, the results presented here suggest that in Arabidopsis, the specific nuclear accumulation of a positive elongation factor initiates differentiation.

Results

MINIYO is required for initiating cell differentiation in the shoot apical meristem

The shoot apical meristem (SAM) of Arabidopsis contains a pool of slow proliferating long-term SCs in the central zone surrounded by faster proliferating transit-amplifying cells. The progeny from these cells is displaced to the periphery of the SAM where it starts to differentiate and generates the aerial organs of the plant in a stereotypic phyllotactic pattern. In an Arabidopsis EMS-mutagenized population we identified the *miniyo-1* (*iyo-1*) mutant that had delayed emergence of the first leaves and altered phyllotaxis (Figure 1A), suggesting that organogenesis in the SAM was perturbed. Moreover, the *iyo-1* mutants had enlarged SAMs, ectopic meristems, and fasciated shoots (Figure 1B-C), which could be due to a defective transition of meristematic cells into differentiation. To clarify the function of

IYO, we analyzed its genetic interaction with *CLV3* and *STM*, two master regulators of SAM development [12, 13]. *CLV3* is expressed in the central zone SCs and is involved in a feedback regulatory loop to maintain a consistent number of SCs [14]. *clv3-2* plants have greatly enlarged SC pools [15] and *iyo-1clv3-2* plants combined the features of the respective single mutants, developing ectopic SAMs, like *iyo-1* plants, each with an enlarged SC population (Figure 1C). The additivity of the phenotypes suggests that *IYO* and *CLV3* have independent functions in the SAM. *STM* is expressed in meristematic cells and is required to prevent their differentiation. Accordingly, *STM* expression is shut down when cells initiate differentiation in the SAM periphery [13]. Reduced *STM* activity in an *stm-6* mutant leads to premature differentiation and SAM termination [16]. In contrast, *iyo-1stm-6* plants had indeterminate SAMs (Figure 1D), suggesting that *IYO* activity is required for the premature differentiation of *stm* mutants. Because *iyo-1* (see below) and *stm-6* are hypomorphic alleles, their epistatic relationship cannot be determined. However, considering the phenotype of *IYO* over expressing plants and the activity domain of *IYO* (see below), we infer that *IYO* is epistatic on *STM*, initiating differentiation in the meristem periphery and turning-off *STM* expression. Consistent with this, the expression of a *pSTM::GUS* reporter, which reproduces endogenous *STM* expression [17], is extended in *iyo-1* shoot apices (Figure 1E). To determine the effects of the *iyo-1* mutation at the gene expression level, we compared the transcriptome of inflorescence apices (comprising the SAM and associated flower primordia) from wild-type (Wt) and *iyo-1* plants. This analysis revealed that *IYO* activity is required in inflorescence apices to shift transcriptional profiles from a program characteristic of undifferentiated cells to a program for flower development (Figure 1F). Among the genes expressed at higher levels in *iyo-1* apices, we found the class

I KNOX tale homeodomain genes *STM*, *KNAT1* and *KNAT6* (Table S1), which are key factors that prevent differentiation of SAM cells [18]. Among the genes that are expressed at lower levels in *iyo-1* inflorescence apices, we found the homeotic flower organ identity genes, which are the master regulators of organ formation in inflorescence meristems [19]. These microarray results support a role of *IYO* in activating cell differentiation and organogenesis in the SAM.

The *iyo-1* mutation causes delayed onset of cell differentiation in all the meristems

Root growth was significantly reduced in *iyo-1* plants (Figure S1), suggesting that *IYO* may also regulate root meristem development. Cell length of mature root cells was not altered in the mutant, indicating that the decrease in root length was due to reduced cell production in the root apical meristem (RAM). Interestingly, the size of the RAM was unchanged relative to Wt plants (Figure S1), implying that cell differentiation rate was also reduced in the mutant, balancing the decrease in cell production. To confirm these results, we analyzed development in the distal end of the RAM, where the transition from precursor cells (columella initials) to their differentiated progeny (columella cells) can be precisely determined based on molecular markers (J2341 marker expression in columella initials and starch accumulation in columella cells [20]). Importantly, the *iyo-1* roots had additional tiers of J2341-positive columella initials between the quiescent center and the first file of starch-containing elongated columella cells (Figure 2A,D), supporting that cell differentiation in the *iyo-1* RAM is delayed. Consistent with a slower rate of differentiation, the expression of J2341 was transiently retained in columella cells.

The conserved role of *IYO* in initiating differentiation in the SAM and the RAM prompted us to test the function in the other plant meristems. The procambium is the meristem that gives rise to the vasculature. In the vascular bundles of the shoot, procambial progeny differentiates internally into xylem cells and peripherally into phloem cells. Histological sections showed that the vascular bundles of *iyo-1* mutants contain more files of procambium cells and fewer mature metaxylem vessels than those of Wt plants (Figure 2B), indicating that the onset of differentiation is also delayed in this meristem. The protoderm is a meristem that generates the epidermis. To compare protoderm development at identical developmental stages, we studied it in cotyledons, which, unlike leaves, are generated synchronously in Wt and *iyo-1* plants (Figure 1A). The tonoplast GFP-δTIP marker allows visualization of vacuole maturation during epidermal cell differentiation [21]. Interestingly, pavement cells in the *iyo-1* epidermis retained tonoplast invaginations until later stages of development, suggesting a slower rate of differentiation (Figure 2C). Moreover, five days after germination, the *iyo-1* cotyledon epidermis still had groups of small brick-like cells resembling protoderm cells, which later entered the stomatal cell lineage, at a stage when the Wt epidermis was fully differentiated. As a consequence of the extra stomata formed, the one-cell spacing rule was disrupted and clusters of 2-8 stomata protruding from the plane of the epidermis developed in *iyo-1* cotyledons (Figure 2C). Clusters of stomata also developed in *iyo-1* leaves, indicating that protoderm differentiation was also perturbed in these organs. These results show that *IYO* participates in initiating cell differentiation in all meristems, most likely at a step prior to cell fate commitment, which is specific for each meristem. This is supported by the observation that, in *iyo-1*

plants, cells expressing SC markers (*pCLV3::GUS*, J2341 or *pTMM::TMM-GFP* [20, 22, 23]) were found outside of the regular temporal and spatial SC niches (Figure 2D). Moreover, extra SAMs, flower meristems, RAMs, meristemoids and embryos developed in the *iyo-1* mutant (Figure 2E), confirming that ectopic SCs are specified. We conclude from these results that *IYO* participates in initiating differentiation of non-committed cells that may retain SC potential.

IYO is essential for cell differentiation

Positional cloning revealed that the *iyo-1* phenotypes were caused by a missense mutation in At4g38440, a gene of unknown function with homologues in all eukaryotic kingdoms. The mutation changes an amino acid that is strictly conserved in all the putative *IYO* orthologues from plants (Figure S2A-B). *iyo-1* is recessive and does not affect transcript accumulation (Figure S2C), suggesting that it is a loss of function allele that may maintain partial activity. This possibility would explain why, though delayed, differentiation of every cell type and organ still occurs in *iyo-1* plants. To test this hypothesis, we characterized the *iyo-2* (SALK_099872) and *iyo-3* (SAIL_692-G12) mutants, which carry T-DNAs insertions in exons and most likely represent null alleles. Heterozygous plants (*iyo-2/IYO* or *iyo-3/IYO*) had phenotypes indistinguishable from Wt plants, whereas homozygous *iyo-2* or *iyo-3* mutants were embryo lethal (Figure 3A and S2D). The size of *iyo-2* and *iyo-3* seeds was severely reduced (Figure 3A and data not shown) implying that endosperm development, which drives seed growth in Arabidopsis [24], is blocked. The endosperm is essential for embryo progression [25], so its defective development in the *iyo-2* and *iyo-3* mutants may cause early embryo arrest. Alternatively,

IYO activity may be required in the embryo for its viability, for instance to maintain active cell proliferation (see discussion). We infer from these results that *iyo-2* and *iyo-3* are null alleles of an essential gene. Interestingly, *iyo-1/iyo-2* or *iyo-1/iyo-3* plants (termed *iyo-1/null* hereafter) displayed stronger defects in differentiation than homozygous *iyo-1* plants (Figure 3B). Embryonic cells remained isodiametric, and the embryos retained a globular shape with radial symmetry, while Wt embryos of the same age (taken from the same silique) had bilateral symmetry and clearly differentiated cell types and embryonic organs (Figure 3B). Moreover, the suspensor of the *iyo-1/null* mutants did not differentiate terminally but instead developed into an ectopic embryo. Cell proliferation was severely reduced but both the primary and the ectopic *iyo-1/null* embryos were viable (Figure 3C). After germination, the *iyo-1/null* plants grew very slowly but could be maintained *in vitro* for several months. The plants developed into callus-like structures with rudimentary leaves that emerged around the whole surface (Figure 3C), suggesting that meristematic activity was not confined to poles as in Wt plants. Reproductive organs were not generated. These exacerbated phenotypes support the notion that *iyo-1* is a hypomorphic allele of *IYO*, an essential factor for initiating differentiation in Arabidopsis.

IYO sustains transcriptional elongation to initiate differentiation

IYO encodes a protein with 24% sequence identity to the mammalian RNAPII Associated Protein 1 (RPAP1) [26] and contains a motif linked to RNA binding that is disrupted in the *iyo-1* allele (Figure S2B). A molecular function in transcriptional regulation would be consistent with its role in initiating differentiation, so we tested whether IYO interacts with RNAPII. In an *in vitro* pull-down assay, IYO bound

specifically to the RNAPII subunit RPB3 (Figure 4A). Moreover, an *in vivo* split YFP assay showed fluorescence reconstitution in the nucleus of cells co-expressing IYO with the RNAPII subunits RPB3 or RPB10 (Figure 4B and S3A-B). Neither the *in vitro* binding nor the *in vivo* YFP reconstitution were affected by the *iyo-1* mutation (Figure 4A and data not shown), which is consistent with the hypomorphic nature of this allele. These results suggest that IYO interacts directly with RNAPII and may regulate its function. Supporting this, the *iyo-1* mutation reduced the levels *in planta* of the largest RNAPII subunit RPB1. Importantly, this reduction was specific for tissues undergoing differentiation (Figure 4C and S3C), where *RPB1* mRNA levels were actually elevated (Figure 4C). This implies that there is an increased rate of RPB1 protein degradation in differentiating tissues of the *iyo-1* mutant. Confirming this, poly-ubiquitinated RPB1 accumulated in *iyo-1* plants in the presence of proteasome inhibitor MG132 (Figure 4D). Poly-ubiquitination and proteasome-mediated degradation of RPB1 are hallmarks of defective transcriptional elongation [27, 28]. Thus, the high levels of these molecular signatures strongly suggest large-scale defects in transcriptional elongation in differentiating tissues of the *iyo-1* mutant. Supporting a positive role of *IYO* in elongation, over-expression of *IYO-GFP* decreased sensitivity to the elongation inhibitor 6-azauracil (Figure 4E). Transcriptional elongation is a highly complex reaction that involves a plethora of elongation factors. Interestingly, *IYO* is highly co-expressed with *ELO3* (Pearson correlation coefficient r=0.76, ACT database), a histone acetyltransferase that is part of a positive elongation complex, the Elongator complex [29]. IYO bound ELO3 *in vitro* (Figure 4F), suggesting that the proteins may cooperate *in vivo*. Supporting this, we found clear evidence of genetic interaction between *IYO* and *ELO3*. While the *elo3-1* mutant has a relatively mild phenotype [30] and *iyo-1* delays but does not

block differentiation, *iyo-1elo3-1* embryos did not differentiate embryonic structures and developed twin embryos from the suspensor (Figure 4G). Once germinated, *iyo-1elo3-1* plants grew as a callus of slowly proliferating undifferentiated cells (Figure 4H). In addition, callus growth was also observed when *iyo-1* was combined with the *elo2-1* and *elo4-1* mutations (Figure 4H), respectively affecting another component and a regulator of Elongator [30]. Taken together, these results suggest that IYO interacts with RNAPII and the Elongator complex to promote transcriptional elongation activity and initiate cell differentiation.

IYO nuclear accumulation is directed to sites of cell differentiation

Northern blot and *in situ* hybridization showed accumulation of *IYO* transcripts in root and shoot apices and in leaf and flower primordia, while tissues containing mainly mature cells had negligible expression (Figure 5A and S2E and data not shown). Consistent with this pattern of transcript accumulation, the *IYO* promoter drove expression of the GUS reporter (*pIYO::GUS*) in the endosperm, the embryo, in meristems and in organ primordia but not in mature cells (Figure 5B-D). In developing leaves *pIYO::GUS* expression followed the reported basipetal gradient of cell maturation [31] while in mature leaves it was found exclusively in the vascular bundles that contain the procambium meristem (Figure 5C). Low *pIYO::GUS* activity was observed in the xylem pole pericycle and in young root primordia (Figure 5D). The activity increased at the base of stage VII primordia, in the cells that first differentiate to drive emergence. After emergence and the establishment of a RAM, the band of strong GUS activity was maintained at the proximal end of the meristem, marking the start of the transition zone where cells enter

differentiation (Figure 5D). The expression of the endogenous transcript and the activity of the promoter fully agree with the genetic data implicating *IYO* in initiating cell differentiation, and would also be compatible with a possible role in maintaining proliferation of undifferentiated cells (see discussion). Moreover, a construct with the *IYO* promoter driving IYO-GFP expression (*pIYO::IYO-GFP*) complemented the *iyo* mutants, indicating that it reproduces the activity of the endogenous gene. To analyze subcellular IYO-GFP distribution, we focused on the root, which has a stereotyped organization and is directly accessible for imaging at single cell-resolution. Consistent with the *pIYO::GUS* results, *pIYO::IYO-GFP* fluorescence was observed in the RAM and in differentiating cells but not in mature cells (Figure 6A and data not shown). Interestingly, the subcellular distribution of IYO-GFP changed as cells entered the transition zone, where cell differentiation is initiated. While in SCs and in transit-amplifying cells at the meristem core IYO-GFP localized diffusely, in cells at the meristem periphery IYO-GFP fluorescence concentrated in the nucleus (Figure 6A-B). To confirm this shift in subcellular distribution in transition cells and analyze IYO-GFP distribution out of the context of the normal domain of *IYO* expression, we used the constitutive *35S* promoter. Moreover, we compared the distribution of IYO-GFP to that of a different GFP fusion (RPB10-GFP) driven by the same 35S promoter. Nuclear *35S::IYO-GFP* signal accumulated in cells at the RAM periphery but not in undifferentiated cells of the meristem core (Figure 6C-D and S4). Moreover, within the RAM, differentiating protophloem cells, which are distinguished by strong propidium iodide staining [32], also accumulated *35S::IYO-GFP* fluorescence in the nucleus (Figure 6E). In mature differentiated cells, where *IYO* is not regularly expressed, *35S::IYO-GFP* fluorescence was nuclear localized (Figure S4). In lateral roots, nuclear

accumulation was first observed in differentiating cells at the base of emerging primordia and later in differentiating cells at the distal and proximal ends of the RAM (Figure S4). Moreover, imaging of the shoot apex revealed that *35S::IYO-GFP* nuclear fluorescence was absent in the SAM core (Figure 6F). In contrast to these results, in plants expressing *35S::RPB10-GFP* there was generalized nuclear fluorescence in every cell of the shoot and root apex, including all the meristematic cells, (Figure 6D-E,G; and S4), a pattern observed when other nuclear GFP fusions are driven by this promoter [33-35]. These results suggest that *cis* elements in the IYO protein sequence direct distinct cytoplasmic/nuclear partitioning of IYO-GFP in undifferentiated and differentiating cells. Given that this is a functional fusion, we infer that the subcellular distribution of endogenous IYO is similarly regulated.

IYO accumulation activates premature cell differentiation

Considering that the transcriptional activity of IYO is involved in initiating differentiation, low nuclear IYO levels in meristematic cells may be necessary to maintain them undifferentiated. Conversely, the increase in nuclear levels at the meristem periphery may serve to switch on differentiation, provided that IYO were the only limiting factor. A prediction from this model is that expressing sufficient amounts of IYO may counterbalance nuclear exclusion in meristematic cells and should then induce premature differentiation. We generated lines expressing HA tagged IYO (IYO-HA) under the control 35S promoter and indeed, only lines expressing high amounts of the fusion protein displayed meristem development phenotypes. Homozygous plants from three independent transgenic lines with the highest IYO-HA levels (*IYO-HAoe* lines) had primary SAMs that

differentiated terminally after producing two small leaves (Figure 7A) and consequently no reproductive organs were generated. *IYO-HAoe* homozygous plants also had smaller primary RAMs, with tracheary elements forming closer to the tip (Figure 7B, arrows). Moreover, the RAMs were sequentially reduced until they were also eventually consumed. Importantly, tracheary elements differentiated in pre-emergence lateral root primordia and root hairs developed in non-elongated cells near the tip (Figure 7C), unequivocal proof of a premature onset of cell differentiation. These results demonstrate that increased IYO levels induce differentiation of meristematic cells, eventually even of the long-term SCs at the core of meristems. Interestingly, the organs formed and the prematurely differentiated cells were correctly patterned (i.e: tracheary elements formed in the center of the primordia and root hairs developed in non-elongated cells of the epidermal layer). We conclude from these results that IYO functions as a universal switch for turning on differentiation after which, patterning cues establish what specific cell types are generated.

Discussion

The evidence presented here suggests that differentiation in Arabidopsis is activated by the specific nuclear accumulation of the positive elongation factor IYO in transition cells. Subcellular redistribution of IYO in those cells may require post-translational modifications. Interestingly, mitosis induces hyperphosphorylation of RPAP1 [36], the putative mammalian homologue of *IYO*, which may be similarly modified. In that scenario, the changes in mitotic activity as cells are displaced from the meristem core [9] may translate into altered IYO phosphorylation and could underlie its redistribution into the nucleus to initiate differentiation. The decreased rates of cell production observed in *iyo*

mutants (i.e. in the *iyo-1* RAM and in *iyo-1/null* embryos and adult plants) suggest that IYO may also be required in undifferentiated cells to promote cell division. In that case, *IYO* could function as a node coordinating the rates of proliferation and differentiation to maintain meristem homeostasis, a notion supported by the balanced reduction of those rates in *iyo* mutants. IYO is primarily cytosolic in undifferentiated cells, so a putative function in cell proliferation could be independent from its transcriptional elongation activity. Interestingly, the Elongator complex has different molecular activities in the cytosol and in the nucleus, regulating protein translation and activating transcription respectively [37, 38]. Moreover, Arabidopsis mutants in the Elongator complex show reduced cell proliferation [30]. An intriguing possibility is that in undifferentiated cells, IYO may recruit the Elongator complex to control protein translation and promote cell proliferation, while in transition cells, IYO recruits the Elongator complex to activate transcription and trigger differentiation.

Although multicellularity and associated with it, cell differentiation, is thought to have evolved independently in the animal and plant lineages [39, 40], there are also examples in animal systems where decisions on differentiation are controlled by transcriptional elongation regulators. In *Drosophila melanogaster* and in *Caenorhabditis elegans* the *Pgc* and PIE-1 proteins bind respectively to the Cdk9 and Cyclin T subunits of the p-TEFb kinase to block general transcriptional elongation and prevent differentiation of primordial germ cells into somatic cells [41, 42]. In vertebrates, repression of transcriptional elongation also preserves the germline from differentiation [43]. Moreover, in mammalian embryonic SCs and in *Drosophila* embryos, productive elongation of developmental regulators is prevented until differentiation is initiated [5, 44]. In all these

cases, repression of transcriptional elongation is associated with the maintenance of an undifferentiated status, and activation with differentiation, a situation similar to what we have unveiled in Arabidopsis. Whether this negative correlation between elongation activity and differentiation is the rule will need to be tested in a larger number of systems. However, it is clear that evolution has repeatedly selected regulators of elongation to mediate the global transcriptional reprogramming that underlies differentiation. An important question to resolve in the future is how the targets of these elongation regulators, and in particular of IYO, are specified. An appealing hypothesis to explore is that the specificity may depend on epigenetic marks associated with the target genes, for instance on the presence of poised RNAPII or of particular chromatin modifications.

Experimental Procedures

For information about the experimental procedures, please see the Supplemental Experimental Procedures.

Acknowledgements

We thank Dr. F. Parcy and Dr. H. Berglund for kindly providing the pBIF and pDEST-TH1 vectors, Dr. R. Simon for the *pCLV3::GUS* and *pSTM::GUS* reporter lines, Dr. F. Sack for the *pTMM::TMM-GFP* line, Dr. J.L. Micol for the *elongata* mutants, and the NASC and ABRC for materials. We also thank P. Paredes for excellent technical assistance. This work was supported, in part, by the Spanish Ministerio de Ciencia e Innovación (BIO2009-10784 and CSD2007-00057 to ER, BFU2009-9783 to CG and BIO2008-03052 to JJSS), the Comunidad de Madrid (P2006/GEN-0191 to ER and CG) and by the USA Department of

Energy (DE-FG03-02ER15295 to NVR). MS, AM and JZ were recipients of postdoctoral contracts from the CSIC I3P programme (cofinanced by the European Social Funds) and Mi.S was recipient of a HSFP long-term fellowship and a Marie Curie Intra-European fellowship.

1. Bernstein, B.E., Mikkelsen, T.S., Xie, X., Kamal, M., Huebert, D.J., Cuff, J., Fry, B., Meissner, A., Wernig, M., Plath, K., Jaenisch, R., Wagschal, A., Feil, R., Schreiber, S.L., and Lander, E.S. (2006). A bivalent chromatin structure marks key developmental genes in embryonic stem cells. Cell *125*, 315-326.
2. Boyer, L.A., Lee, T.I., Cole, M.F., Johnstone, S.E., Levine, S.S., Zucker, J.P., Guenther, M.G., Kumar, R.M., Murray, H.L., Jenner, R.G., Gifford, D.K., Melton, D.A., Jaenisch, R., and Young, R.A. (2005). Core transcriptional regulatory circuitry in human embryonic stem cells. Cell *122*, 947-956.
3. Brookes, E., and Pombo, A. (2009). Modifications of RNA polymerase II are pivotal in regulating gene expression states. EMBO Rep *10*, 1213-1219.
4. Guenther, M.G., Levine, S.S., Boyer, L.A., Jaenisch, R., and Young, R.A. (2007). A chromatin landmark and transcription initiation at most promoters in human cells. Cell *130*, 77-88.
5. Stock, J.K., Giadrossi, S., Casanova, M., Brookes, E., Vidal, M., Koseki, H., Brockdorff, N., Fisher, A.G., and Pombo, A. (2007). Ring1-mediated ubiquitination of H2A restrains poised RNA polymerase II at bivalent genes in mouse ES cells. Nat Cell Biol *9*, 1428-1435.
6. Iyer-Pascuzzi, A.S., and Benfey, P.N. (2009). Transcriptional networks in root cell fate specification. Biochim Biophys Acta *1789*, 315-325.
7. Dello Ioio, R., Nakamura, K., Moubayidin, L., Perilli, S., Taniguchi, M., Morita, M.T., Aoyama, T., Costantino, P., and Sabatini, S. (2008). A genetic framework for the control of cell division and differentiation in the root meristem. Science *322*, 1380-1384.
8. Reinhardt, D., Pesce, E.R., Stieger, P., Mandel, T., Baltensperger, K., Bennett, M., Traas, J., Friml, J., and Kuhlemeier, C. (2003). Regulation of phyllotaxis by polar auxin transport. Nature *426*, 255-260.
9. Bennett, T., and Scheres, B. (2010). Root development-two meristems for the price of one? Curr Top Dev Biol *91*, 67-102.
10. Niwa, H. (2007). Open conformation chromatin and pluripotency. Genes Dev *21*, 2671-2676.

11. Gaspar-Maia, A., Alajem, A., Polesso, F., Sridharan, R., Mason, M.J., Heidersbach, A., Ramalho-Santos, J., McManus, M.T., Plath, K., Meshorer, E., and Ramalho-Santos, M. (2009). Chd1 regulates open chromatin and pluripotency of embryonic stem cells. Nature *460*, 863-868.
12. Fletcher, J.C. (2002). Shoot and floral meristem maintenance in arabidopsis. Annu Rev Plant Biol *53*, 45-66.
13. Long, J.A., Moan, E.I., Medford, J.I., and Barton, M.K. (1996). A member of the KNOTTED class of homeodomain proteins encoded by the STM gene of Arabidopsis. Nature *379*, 66-69.
14. Brand, U., Fletcher, J.C., Hobe, M., Meyerowitz, E.M., and Simon, R. (2000). Dependence of stem cell fate in Arabidopsis on a feedback loop regulated by CLV3 activity. Science *289*, 617-619.
15. Fletcher, J.C., Brand, U., Running, M.P., Simon, R., and Meyerowitz, E.M. (1999). Signaling of cell fate decisions by CLAVATA3 in Arabidopsis shoot meristems. Science *283*, 1911-1914.
16. Endrizzi, K., Moussian, B., Haecker, A., Levin, J.Z., and Laux, T. (1996). The SHOOT MERISTEMLESS gene is required for maintenance of undifferentiated cells in Arabidopsis shoot and floral meristems and acts at a different regulatory level than the meristem genes WUSCHEL and ZWILLE. Plant J *10*, 967-979.
17. Kirch, T., Simon, R., Grunewald, M., and Werr, W. (2003). The DORNROSCHEN/ENHANCER OF SHOOT REGENERATION1 gene of Arabidopsis acts in the control of meristem ccll fate and lateral organ development. Plant Cell *15*, 694-705.
18. Hay, A., and Tsiantis, M. (2009). A KNOX family TALE. Curr Opin Plant Biol *12*, 593-598.
19. Sablowski, R. (2010). Genes and functions controlled by floral organ identity genes. Semin Cell Dev Biol *21*, 94-99.
20. Friml, J., Benkova, E., Blilou, I., Wisniewska, J., Hamann, T., Ljung, K., Woody, S., Sandberg, G., Scheres, B., Jurgens, G., and Palme, K. (2002). AtPIN4 mediates sink-driven auxin gradients and root patterning in Arabidopsis. Cell *108*, 661-673.
21. Saito, C., Ueda, T., Abe, H., Wada, Y., Kuroiwa, T., Hisada, A., Furuya, M., and Nakano, A. (2002). A complex and mobile structure forms a distinct subregion within the continuous vacuolar membrane in young cotyledons of Arabidopsis. Plant J *29*, 245-255.
22. Brand, U., Grunewald, M., Hobe, M., and Simon, R. (2002). Regulation of CLV3 expression by two homeobox genes in Arabidopsis. Plant Physiol *129*, 565-575.
23. Nadeau, J.A., and Sack, F.D. (2002). Control of stomatal distribution on the Arabidopsis leaf surface. Science *296*, 1697-1700.
24. Sundaresan, V. (2005). Control of seed size in plants. Proc Natl Acad Sci U S A *102*, 17887-17888.
25. Nowack, M.K., Grini, P.E., Jakoby, M.J., Lafos, M., Koncz, C., and Schnittger, A. (2006). A positive signal from the fertilization of the egg cell sets off endosperm proliferation in angiosperm embryogenesis. Nat Genet *38*, 63-67.
26. Jeronimo, C., Langelier, M.F., Zeghouf, M., Cojocaru, M., Bergeron, D., Baali, D., Forget, D., Mnaimneh, S., Davierwala, A.P., Pootoolal, J., Chandy, M., Canadien,

V., Beattie, B.K., Richards, D.P., Workman, J.L., Hughes, T.R., Greenblatt, J., and Coulombe, B. (2004). RPAP1, a novel human RNA polymerase II-associated protein affinity purified with recombinant wild-type and mutated polymerase subunits. Mol Cell Biol *24*, 7043-7058.

27. Anindya, R., Aygun, O., and Svejstrup, J.Q. (2007). Damage-induced ubiquitylation of human RNA polymerase II by the ubiquitin ligase Nedd4, but not Cockayne syndrome proteins or BRCA1. Mol Cell *28*, 386-397.
28. Somesh, B.P., Reid, J., Liu, W.F., Sogaard, T.M., Erdjument-Bromage, H., Tempst, P., and Svejstrup, J.Q. (2005). Multiple mechanisms confining RNA polymerase II ubiquitylation to polymerases undergoing transcriptional arrest. Cell *121*, 913-923.
29. Nelissen, H., De Groeve, S., Fleury, D., Neyt, P., Bruno, L., Bitonti, M.B., Vandenbussche, F., Van der Straeten, D., Yamaguchi, T., Tsukaya, H., Witters, E., De Jaeger, G., Houben, A., and Van Lijsebettens, M. (2010). Plant Elongator regulates auxin-related genes during RNA polymerase II transcription elongation. Proc Natl Acad Sci U S A *107*, 1678-1683.
30. Nelissen, H., Fleury, D., Bruno, L., Robles, P., De Veylder, L., Traas, J., Micol, J.L., Van Montagu, M., Inze, D., and Van Lijsebettens, M. (2005). The elongata mutants identify a functional Elongator complex in plants with a role in cell proliferation during organ growth. Proc Natl Acad Sci U S A *102*, 7754-7759.
31. Donnelly, P.M., Bonetta, D., Tsukaya, H., Dengler, R.E., and Dengler, N.G. (1999). Cell cycling and cell enlargement in developing leaves of Arabidopsis. Dev Biol *215*, 407-419.
32. Truernit, E., Bauby, H., Dubreucq, B., Grandjean, O., Runions, J., Barthelemy, J., and Palauqui, J.C. (2008). High-resolution whole-mount imaging of three-dimensional tissue organization and gene expression enables the study of Phloem development and structure in Arabidopsis. Plant Cell *20*, 1494-1503.
33. Coates, J.C., Laplaze, L., and Haseloff, J. (2006). Armadillo-related proteins promote lateral root development in Arabidopsis. Proc Natl Acad Sci U S A *103*, 1621-1626.
34. Lee, B.H., Kapoor, A., Zhu, J., and Zhu, J.K. (2006). STABILIZED1, a stress-upregulated nuclear protein, is required for pre-mRNA splicing, mRNA turnover, and stress tolerance in Arabidopsis. Plant Cell *18*, 1736-1749.
35. Wildwater, M., Campilho, A., Perez-Perez, J.M., Heidstra, R., Blilou, I., Korthout, H., Chatterjee, J., Mariconti, L., Gruissem, W., and Scheres, B. (2005). The RETINOBLASTOMA-RELATED gene regulates stem cell maintenance in Arabidopsis roots. Cell *123*, 1337-1349.
36. Daub, H., Olsen, J.V., Bairlein, M., Gnad, F., Oppermann, F.S., Korner, R., Greff, Z., Keri, G., Stemmann, O., and Mann, M. (2008). Kinase-selective enrichment enables quantitative phosphoproteomics of the kinome across the cell cycle. Mol Cell *31*, 438-448.
37. Mehlgarten, C., Jablonowski, D., Wrackmeyer, U., Tschitschmann, S., Sondermann, D., Jager, G., Gong, Z., Bystrom, A.S., Schaffrath, R., and Breunig, K.D. (2010). Elongator function in tRNA wobble uridine modification is conserved between yeast and plants. Mol Microbiol *76*, 1082-1094.

38. Versees, W., De Groeve, S., and Van Lijsebettens, M. (2010). Elongator, a conserved multitasking complex? Mol Microbiol *76*, 1065-1069.
39. Birnbaum, K.D., and Sanchez Alvarado, A. (2008). Slicing across kingdoms: regeneration in plants and animals. Cell *132*, 697-710.
40. Meyerowitz, E.M. (2002). Plants compared to animals: the broadest comparative study of development. Science *295*, 1482-1485.
41. Hanyu-Nakamura, K., Sonobe-Nojima, H., Tanigawa, A., Lasko, P., and Nakamura, A. (2008). Drosophila Pgc protein inhibits P-TEFb recruitment to chromatin in primordial germ cells. Nature *451*, 730-733.
42. Zhang, F., Barboric, M., Blackwell, T.K., and Peterlin, B.M. (2003). A model of repression: CTD analogs and PIE-1 inhibit transcriptional elongation by P-TEFb. Genes Dev *17*, 748-758.
43. Venkatarama, T., Lai, F., Luo, X., Zhou, Y., Newman, K., and King, M.L. (2010). Repression of zygotic gene expression in the Xenopus germline. Development *137*, 651-660.
44. Zeitlinger, J., Stark, A., Kellis, M., Hong, J.W., Nechaev, S., Adelman, K., Levine, M., and Young, R.A. (2007). RNA polymerase stalling at developmental control genes in the Drosophila melanogaster embryo. Nat Genet *39*, 1512-1516.
45. Malamy, J.E., and Benfey, P.N. (1997). Organization and cell differentiation in lateral roots of Arabidopsis thaliana. Development *124*, 33-44.

Figure 1. *IYO* is required for differentiation in the SAM periphery. (A) Leaf emergence in plants grown *in vitro* for 9 days or *in soil* for the indicated days. Bar: 1 mm. (B) Histological sections of vegetative (14 day-old plants) and reproductive (21 day-old plants) SAMs. Bar: 50 ⌈m. (C) Scanning electron micrographs of the SAM (23 day-old plants) and light images of shoots (30 day-old plants) from Wt, *iyo-1*, *clv3-2* and *iyo-1clv3-2* plants. Meristematic cells are pseudocolored in green and flower primordia in light brown for clarity. Arrow: ectopic SAM. (D) Images of determinate inflorescence apices in the *stm-6* mutant and indeterminate apices, with callus overgrowths, in *iyo-1stm-6* plants. (E) GUS staining pattern in 8 day-old Wt and *iyo-1* seedlings transgenic for *pSTM::GUS*. Bar: 200 μm. (F) Graphical display of microarray expression data (log_2 of the expression ratio) in flowers versus callus (Flower/callus) and flowers versus cell culture (Flower/cell cult) for

the 380 most significantly ($p \leq 0.00066388$) repressed and the 380 most significantly ($p \leq 0.00015957$) induced genes in Wt versus *iyo-1* (Wt/iyo) inflorescence apices. See also Table S1.

Figure 2. The onset of differentiation is delayed in all *iyo-1* meristems. (A) Root tips from 5 day-old plants stained with lugol. Brackets: columella initials. Bar: 25 μm. (B) Histological cross sections through the basal internodes from primary inflorescences (which develop simultaneously in *iyo-1* and Wt) of 35 day-old plants. Images of whole sections (Bar: 200 μm), vascular bundles (Bar: 50 μm) and close ups of the framed regions are shown. Black dots mark files of procambium cells. P: Phloem cell; X: Xylem cell. (C) Time series of adaxial epidermis development in cotyledon from Wt and *iyo-1* plants expressing a *35S::GFP-δTIP* tonoplast marker (green signal). The age of the plants is indicated in the panels. Arrows: Undifferentiated protoderm cells. Arrowhead: stomatal cluster. Bar: 50 μm and 10 μm (panel on the lower right side). (D) Expression of SC markers in the *iyo-1* plants. Insets: expression in Wt plants at the same developmental stage. *pCLV3::GUS*: 21 day-old plants (Bar: 2.5 mm) and developing flowers (Bar: 100 μm); J2341: root tips from 5 day-old plants (Bar: 50 μM); *pTMM::TMM-GFP*: cotyledon epidermis from 6 day-old plants (Bar: 25 μm). (E) Scanning electron micrograph of the shoot apex from an 11-day-old *iyo-1* plant. Arrow: ectopic SAM (100% of the plants developed ectopic SAMs, n= 108). Bar: 50 μm. (F) Compound (triple) *iyo-1* flower (on average more than one duplicated flower per plant, n=108 plants). (G) Image of an *iyo-1* root with two RAMs expressing the *pCYCB1;1::GUS* marker (in 17-day old *iyo-1* plants,

57% displayed at least one root with double RAMs, n= 145 plants). Bar: 25 μm. (H) Twin embryos in an *iyo-1* seed (2 cases of duplicated embryos were found in *iyo-1* seeds and none in Wt seeds, approximately 300 seeds analyzed for each genotype). Bar: 25 μm. See also figure S1.

Figure 3. *IYO* is an essential factor for differentiation. (A) Nomarski images of cleared ovules from siliques of heterozygous *iyo-2/IYO* plants. The *iyo-2* (bottom panels) and the corresponding Wt or heterozygous plants (top panels) from the same silique are shown. The stage of the Wt or heterozygous embryos is indicated. Similar defects in endosperm and embryo development were observed in the *iyo-3* mutant. Bar: 25 μm. (B) Embryos from the F1 cross between *iyo-1* homozygous mutants and heterozygous *iyo-2/IYO* or *iyo-3/IYO* plants. Stages of embryogenesis are classified according to the *iyo-1/IYO* embryos in the same silique. Arrows: periclinal divisions in the suspensor. Arrowhead: ectopic embryo (73% of the *iyo-1*/*null* seeds developed ectopic embryos from the suspensor, n=43). The insets in the lower panels show the *iyo/null* embryos at the same magnification as the corresponding mature *iyo-1/IYO* embryo. Bar: 25 μm. (C) Developmental time series of *iyo-1/iyo-2* and *iyo-1/IYO* progeny derived from the same plant. The age of the plants is indicated in the panels. Arrowhead: ectopic embryo. Bar: 500 μm. See also Figure S2.

Figure 4. IYO activates transcriptional elongation to initiate differentiation. (A) *In vitro* RPB3 pull down assay. (B) YFP reconstitution in the nucleus of *Nicotiana*

benthamiana plants expressing split nYFP-IYO and RPB3-cYFP or nYFP-IYO and RPB10-cYFP. Arrow: absence of fluorescence in the nucleolus. Bars: 50 μm and 10 μm (right panels). (C) Levels of the elongating form of RPB1 (Ser2P, left panel) and the *RPB1* mRNA levels (right panel) were determined in leaf primordia < 2 mm in length (LP) and in mature fully elongated leaves (ML) from plants grown *in vitro* for 9 or 16 days. Loading controls are the Rubisco large subunit (RbcL) and rRNA, respectively. (D) Whole protein extracts (input) from seedlings treated with (+) or without (-) 20 μM MG132 were immunoprecipitated with 8WG16 antibodies (IP) and the presence of RPB1 and ubiquitinated proteins was detected with 8WG16 or anti-ubiquitin antibodies respectively, in wild type (W) and *iyo-1* (i) plants. (E) Seedlings grown in the presence of different concentrations (μM) of 6-azauracil (6-AU) for 11 days. (F) *in vitro* ELO3 pull-down assay. An unrelated fusion (MBP-JAZ8) was used as an additional negative control. (G) *iyo-1elo3-1* mature embryo. Arrowhead: ectopic embryo forms in the suspensor. Bar: 25 μm. (H) *iyo-1elo3-1*, *iyo-1elo2-1*, and *iyo-1elo4-1* plants grown *in vitro* for 6 weeks. Insets: development of single mutants for comparison. Bar: 2.5 mm. See also figure S3.

Figure 5. *IYO* is expressed in meristems and organ primordia. (A) *In situ* hybridization of 22 day-old Wt inflorescence apex with a *IYO* antisense probe. Inset: sense probe control hybridization. Bar: 100 μm. (B-D) GUS staining pattern of *pIYO::GUS* plants are shown. Bar: 50 μm (developing seed), 100 μm (embryo), 2 mm (8 day-old seedling), 50 μm (SAM from 5 day-old seedling), 200 μm (developing leaves), 50 μm (lateral root

primordia and lateral roots). Stages of root primordia development are as previously defined [45]. GUS reaction time in (B-C) was 14 hours and in (D) 1 hour.

Figure 6. Redistribution of IYO-GFP to the nucleus in cells at the meristem boundaries. (A) Pattern of *pIYO::GUS* staining and *pIYO::IYO-GFP* fluorescence signal distribution in roots. Bar: 25 μm. TZ: transition zone. EZ: elongation zone. (B) Detail of the subcellular *pIYO::IYO-GFP* fluorescence distribution in the epidermal layer of the root. Arrowhead: first proximal cell showing fluorescence accumulation in the nucleus. Bar: 25 μm. (C) Images of roots from *35S::IYO-GFP* and *35S::RPB10-GFP* plants. Bar: 100 μm (D) Details of subcellular fluorescence distribution in the distal (left panel) and proximal (right panel) ends of the RAM from *35S::IYO-GFP* plants. Insets: images from *35S::RPB10-GFP* plants at the same stage. First proximal cells showing nuclear fluorescence accumulation in epidermis (asterisks) and cortex (dots) files are labeled. Bar: 50 μm. (E) Image of the RAM from a *35S::IYO-GFP* plant in the focal plane of a differentiating protophloem file. A close-up of the region framed is shown in the two panels on the right. Middle panel: propidium iodide staining. Right panel: overlay of propidium iodide staining and GFP fluorescence. Bar: 50 μm. (F) Image from shoot apices. The frame highlights the SAM core. Bar: 50 μm. See also Figure S4.

Figure 7. IYO is a limiting factor for initiating differentiation of meristematic cells. (A) Images of 10 day-old seedlings and close-up of the SAM in Wt and *IYO-HAoe* plants. Bar: 2 mm. Emerged leaves are numbered. (B) Nomarski images of roots from *IYO-HAoe*

plants at different days after germination. The dot marks the position of the quiescent center and the arrowhead the proximal limit of the RAM. The insets show the size of the RAM in roots of Wt plants of the same age grown in the same plates. Bar: 50 μm. Arrows: tracheary elements. (C) Premature differentiation of tracheary elements in lateral root primordia (arrows) and of root hairs in non-elongated epidermal cells from lateral roots (asterisks). Bar: 50 μm.

Figure 1

Click here to download high resolution image

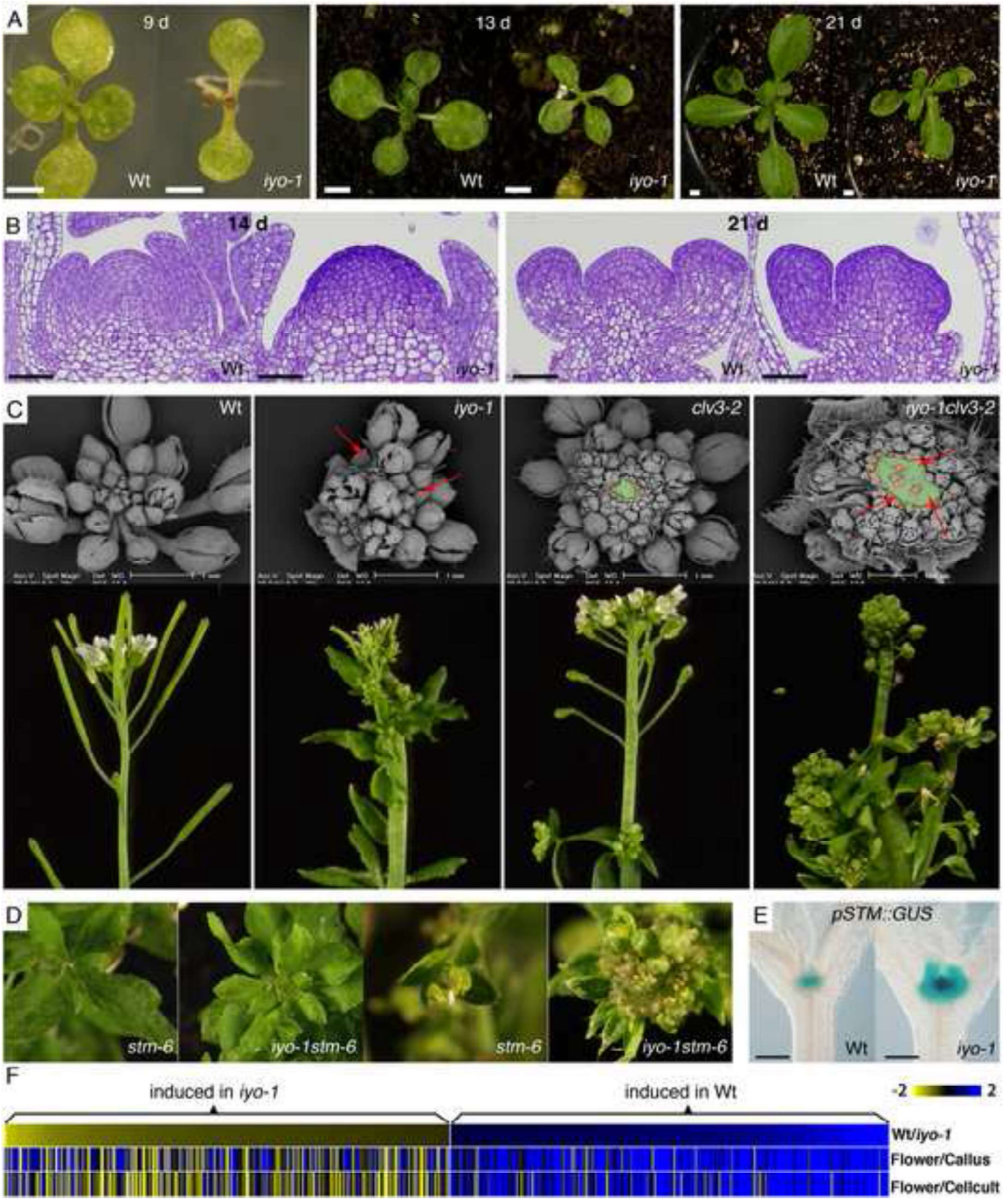

Figure 2

Click here to download high resolution image

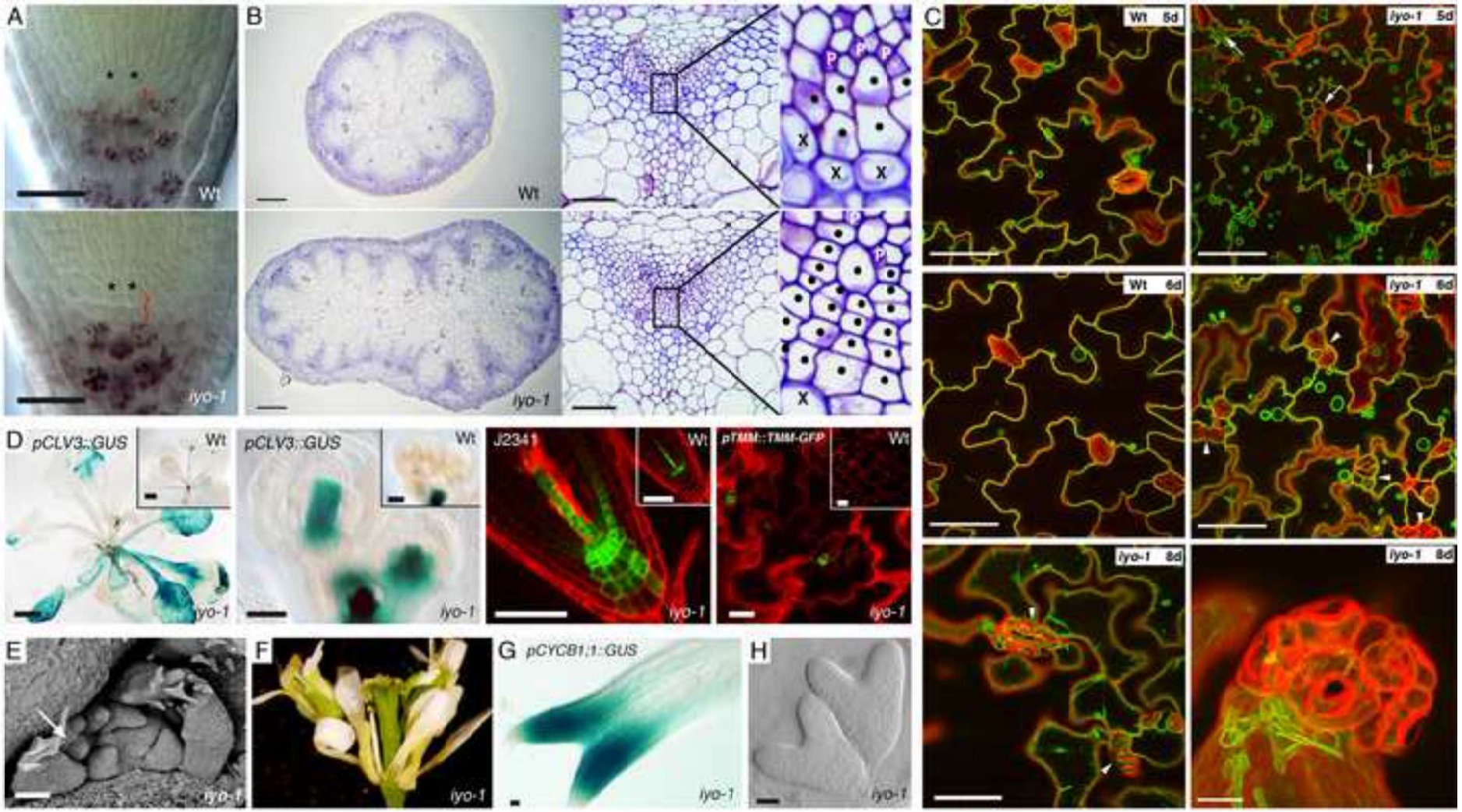

Figure 3

Click here to download high resolution image

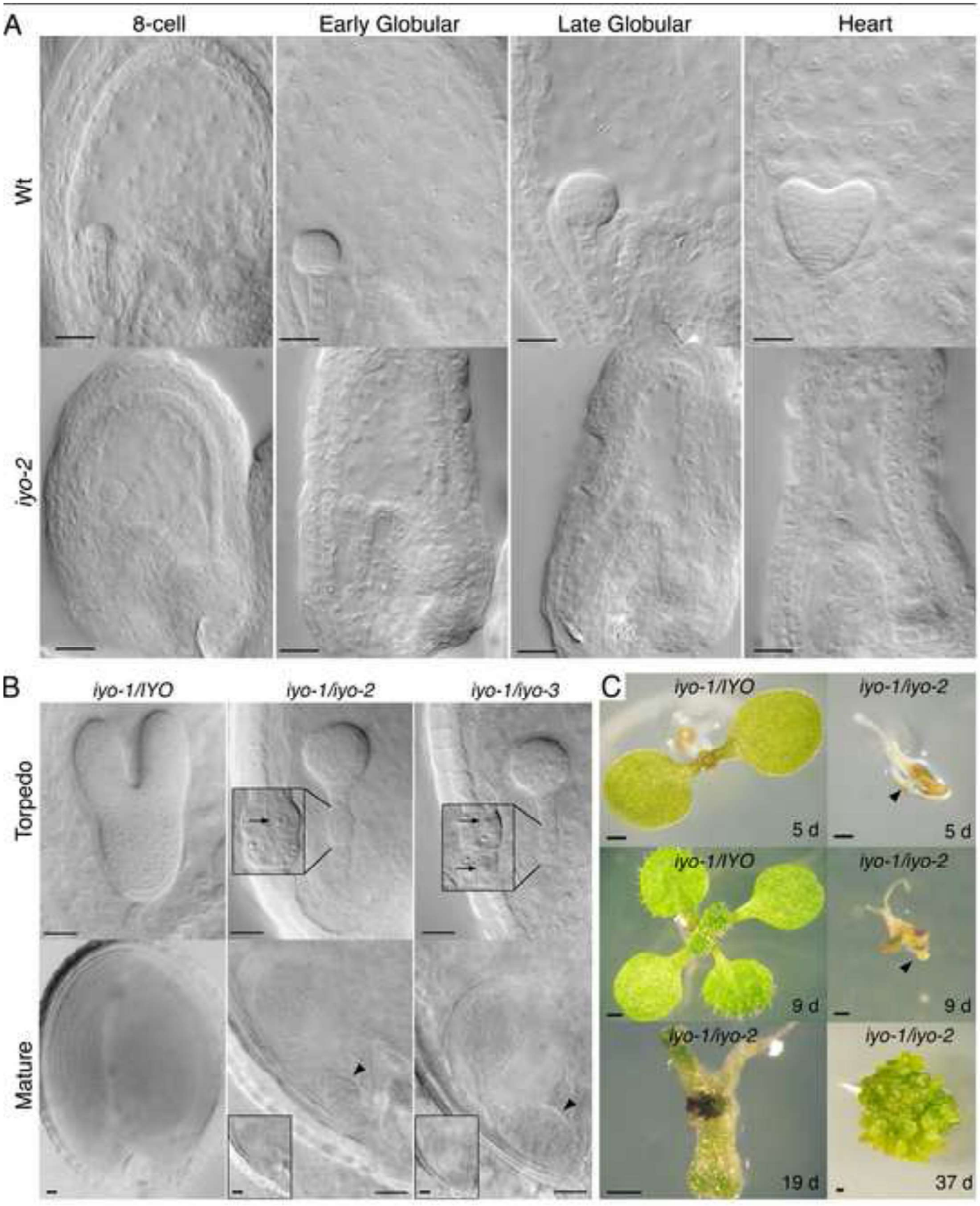

Figure 4

Click here to download high resolution image

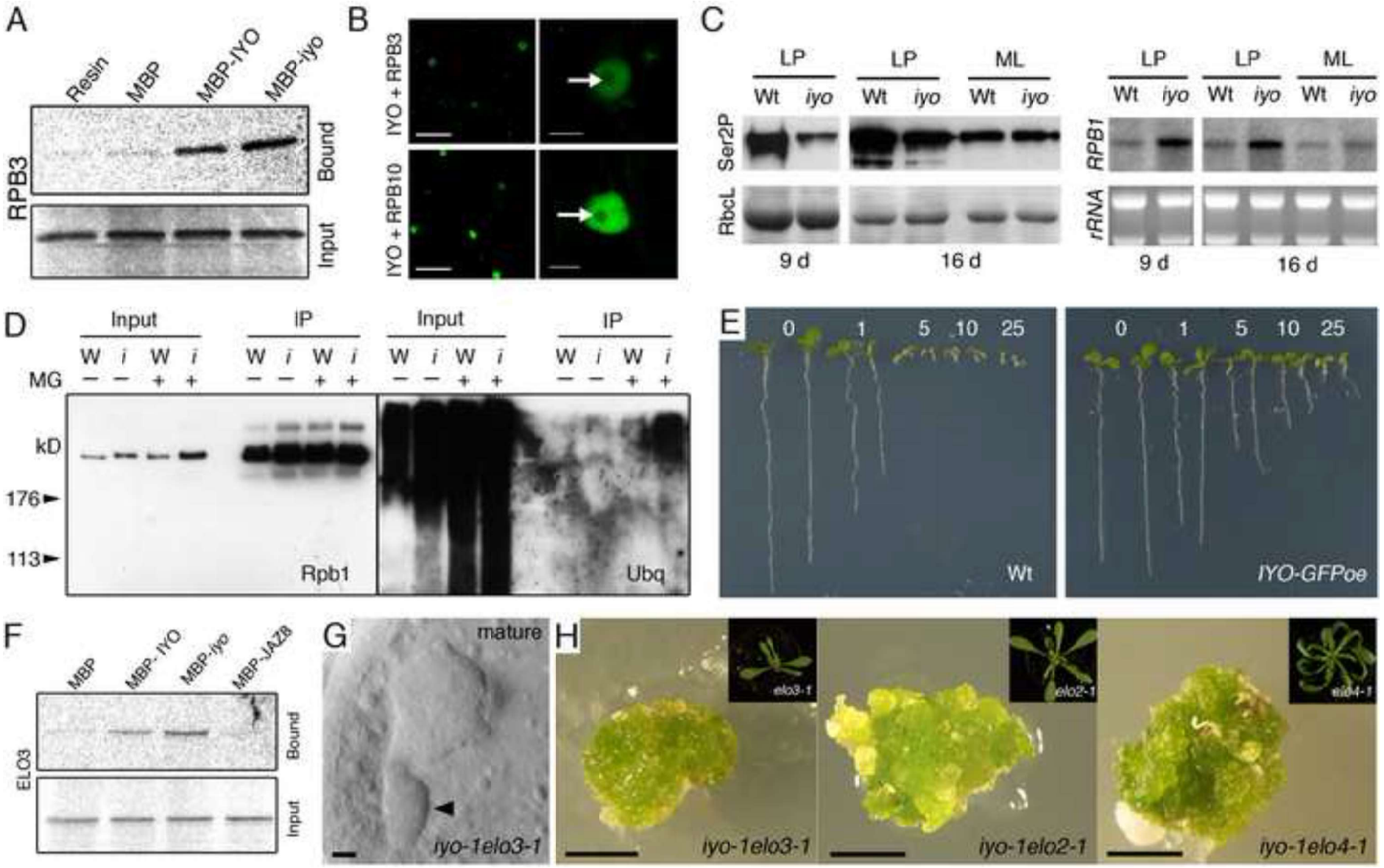

Figure 5

Click here to download high resolution image

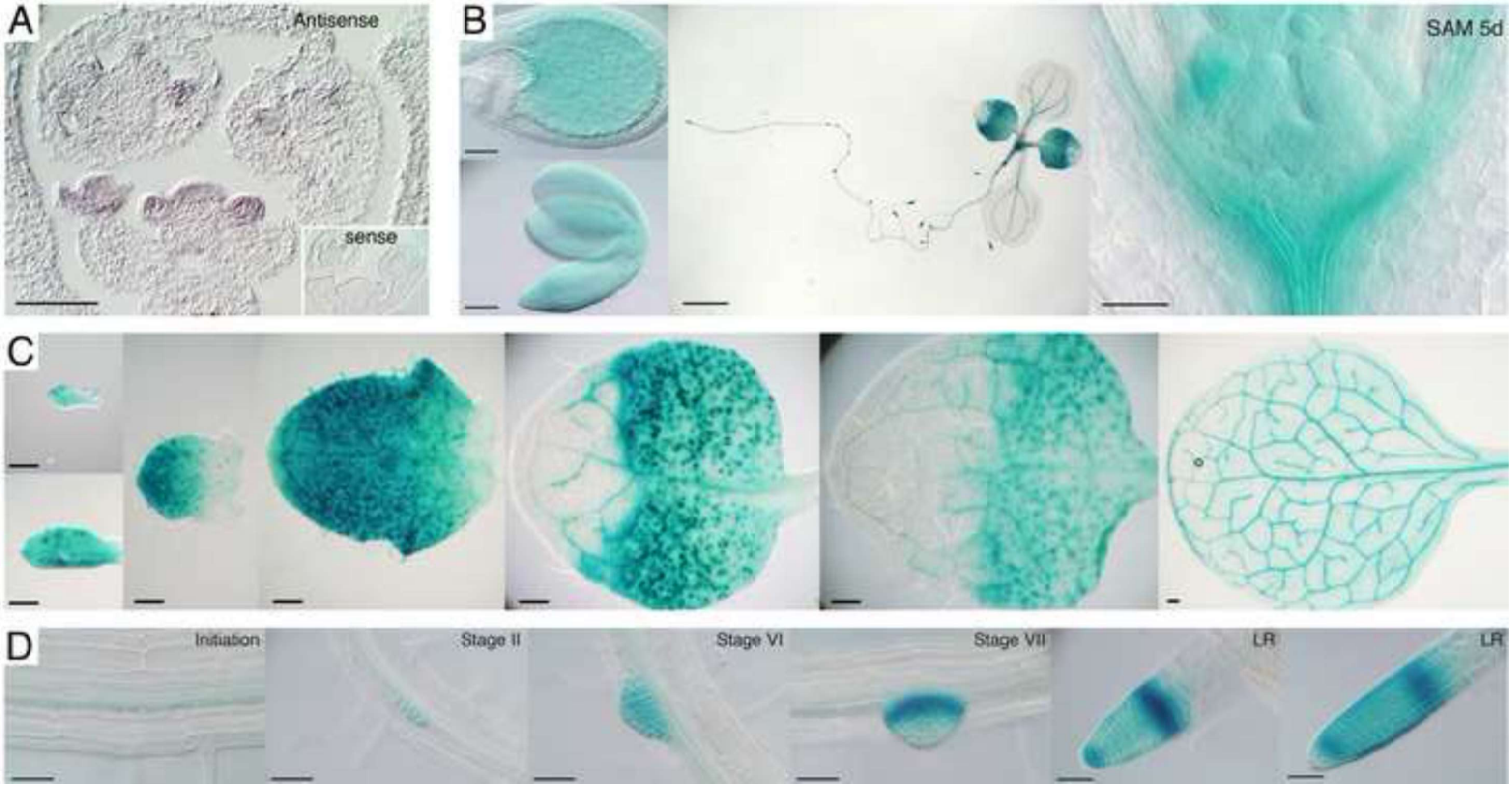

Figure 6

Click here to download high resolution image

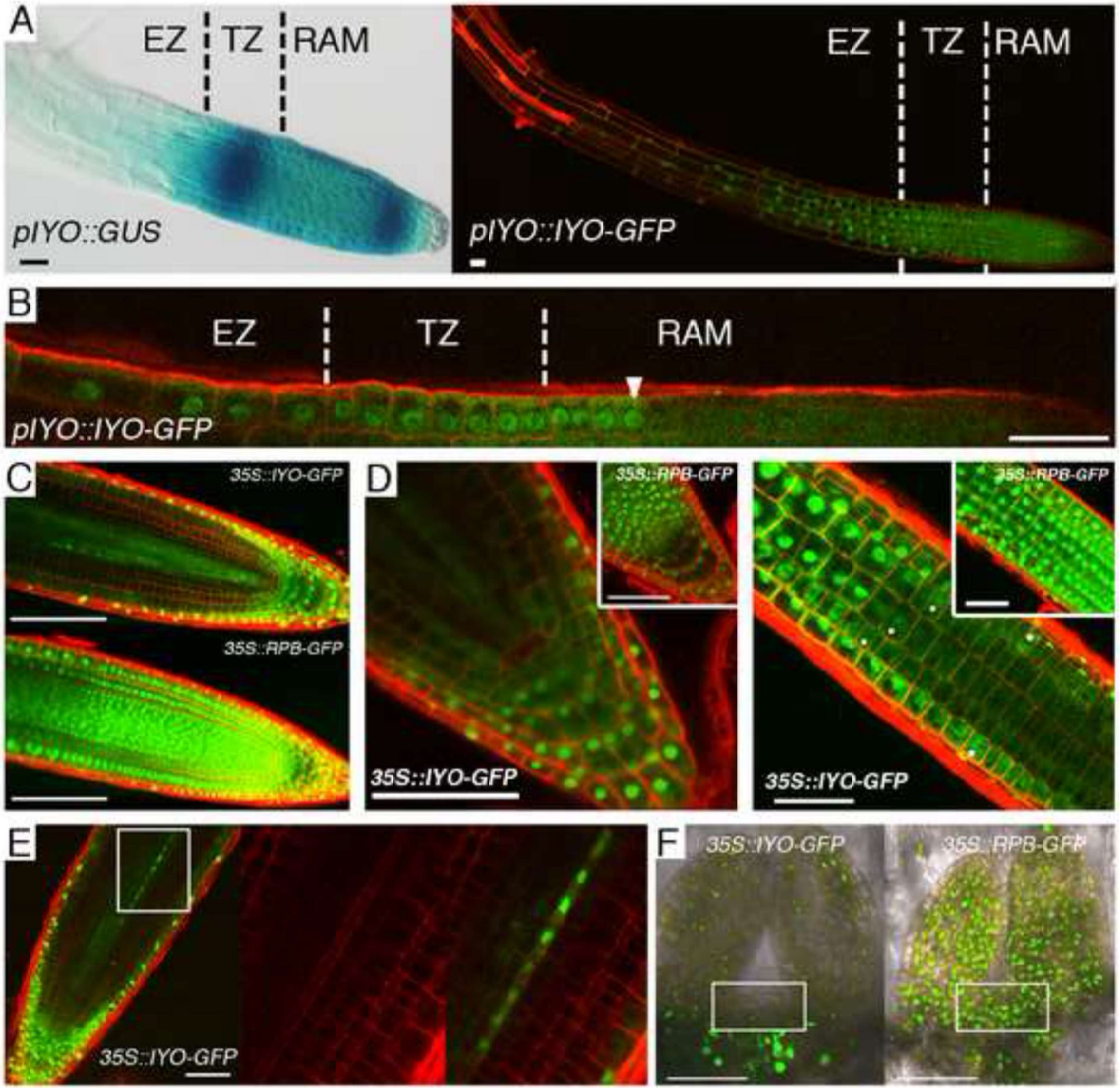

Figure 7

Click here to download high resolution image

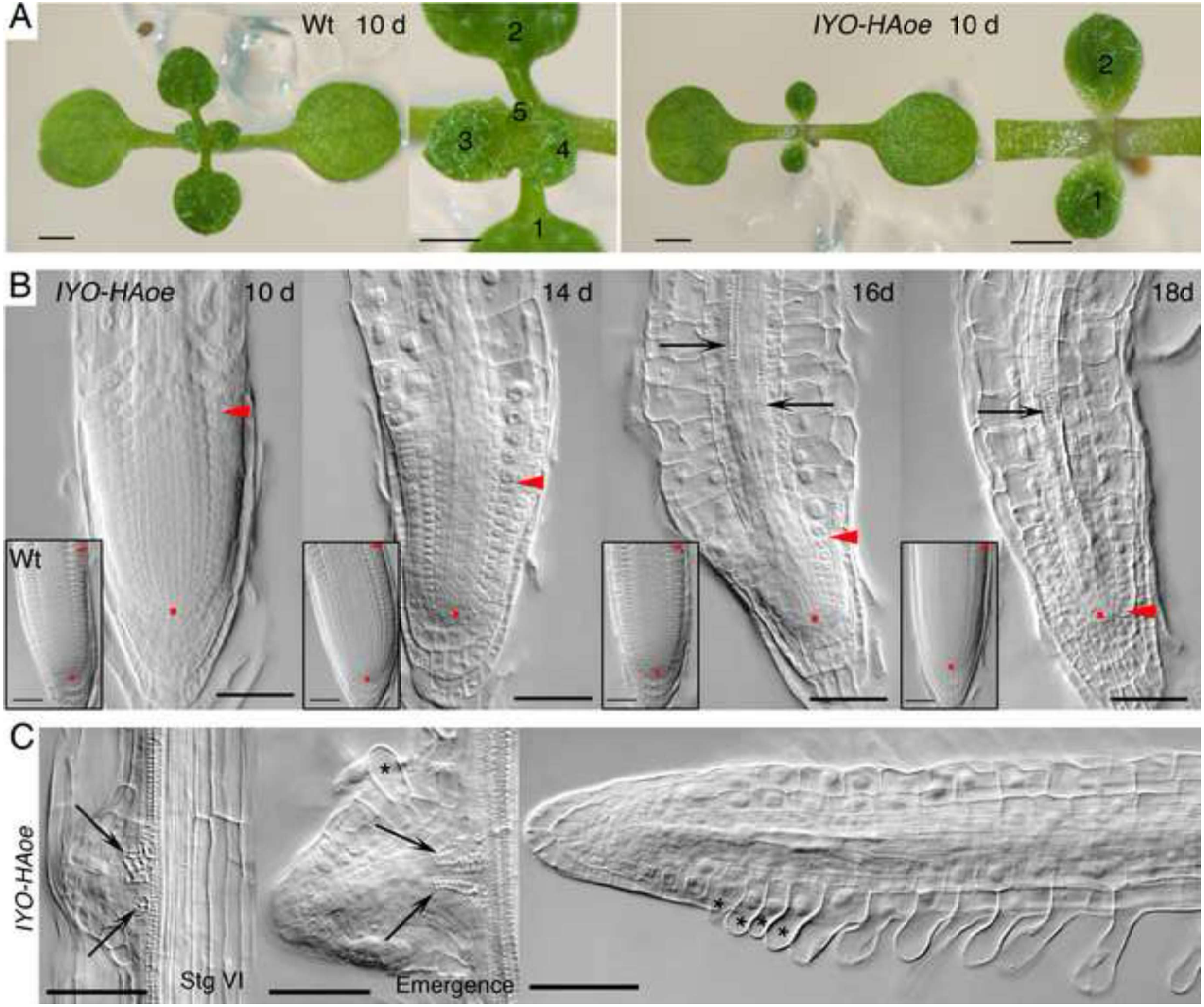

Inventory of Supplemental Information:

Figure S1: Root parameters in Wt and *iyo-1* plants (Related to Figure 2).

Figure S2: *iyo-1* mapping information, sequence comparisons and mRNA expression (Related to Figure 3).

Figure S3: Split YFP reconstitution assays with the negative controls used (Related to Figure 4).

Figure S4: Comparison of *35S:IYO-GFP* and *35S::RPB10-GFP* fluorescence distribution during lateral root development (Related to Figure 6).

Table S1: Expression of a selected list of genes in the microarray experiments performed (Related to Figure 1).

Supplemental Experimental Procedures.

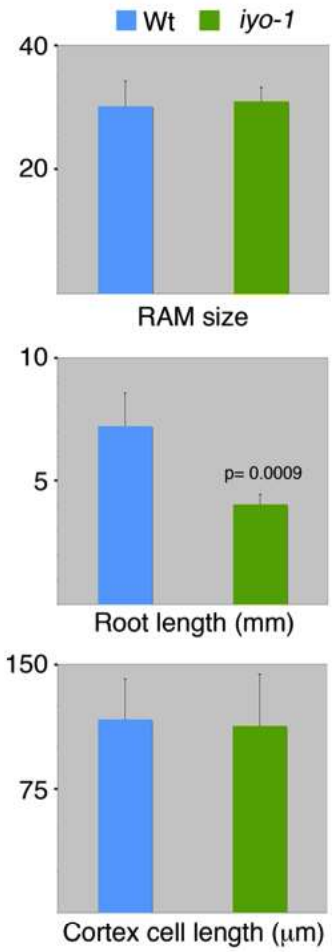

Figure S1. Reduced cell proliferation and cell differentiation rates in the *iyo-1* RAM (Related to Figure 2). The mean RAM size (measured as the number of meristematic cells in a cortex file), root length and mature cortex cell length in 5 day-old Wt and *iyo-1* seedlings is shown. Error bars: SD; p-value, two-tailed unpaired Student's *t* test. The means from two independent experiments are shown.

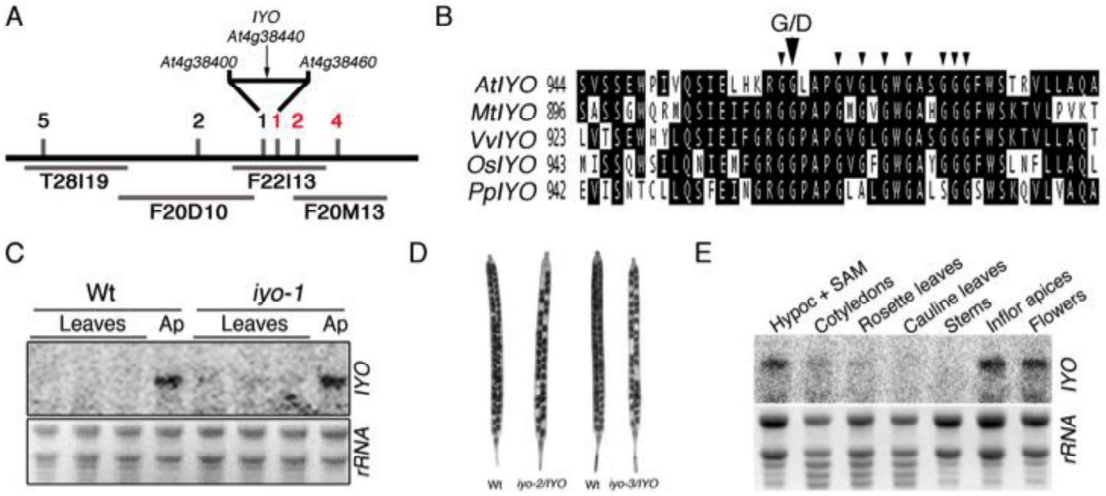

Figure S2. Identification of *MINIYO* (Related to Figure 3). (A) Mapping summary showing the number of recombinant chromosomes in a total of over 1500 mutant plants genotyped. (B) Alignment of the region of IYO containing the *iyo-1* mutation (G/D amino acid substitution) that disrupts an RGG box that has been linked to RNA binding [1]. Small arrowheads: conserved glycines. At: *Arabidopsis thaliana*; Mt: *Medicago truncatula*; Vv: *Vitis vinifera*, Os: *Oryza sativa*; Pp: *Physcomitrella patents*. (C) Total RNA extracted from shoot apices (Ap) and mature leaves (Leaves) from 22 day-old Wt and *iyo-1* plants was analyzed by northern blot with a *IYO* probe. (D) Images of seed set in siliques cleared with ethanol from Wt, *iyo-2/IYO* and *iyo-3/IYO* plants grown in the same conditions. (E) Northern blot hybridization of RNA extracted from the indicated tissue samples. The aerial tissue from 7 day-old Wt seedlings was separated into hypocotyl plus SAM (Hypoc+SAM) and cotyledons. Mature rosette and cauline leaves, stems, inflorescence apices and developing flower samples were from 30 day-old Wt plants.

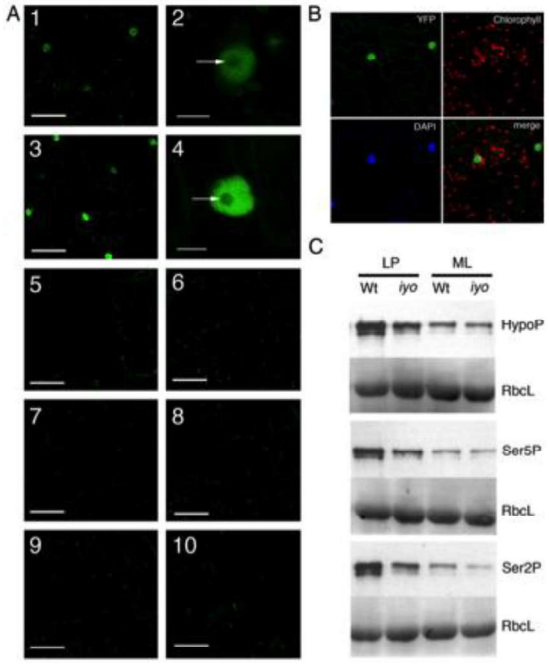

Figure S3. IYO interacts *in vivo* with RNAPII (Related to Figure 4). (A) Bimolecular fluorescence complementation in the nucleus of split YFP expressed in *Nicotiana benthamiana*. Panel 1 and 2: nYFP-IYO and RPB3-cYFP; 3 and 4: nYFP-IYO and RPB10-cYFP; arrows in 2 and 4 show the lack of reconstituted YFP in the nucleolus. 5: background autofluorescence in untransformed leaf; 6: IYO-nYFP and RPB3-cYFP; 7: nYFP-IYO and MYC2-cYFP; 8: RPB3-nYFP and cYFP-IYO; 9: RPB3-nYFP and IYO-cYFP; 10: RPB10-nYFP and RPB3-cYFP. Bars: 50 ⌈m (panels 1, 3, 5-8); 10 ⌈m (panels 2-4). (B) Reconstituted YFP (nYFP-IYO and RPB10-cYFP) colocalizes with DAPI in nuclei of *Nicotiana benthamiana*. Chlorophyll: chlorophyll autofluorescence. Bar: 50 ⌈m. (C) The levels of the preinitiation form (HypoP), the initiating form (Ser5P) and the elongating form of RPB1 (Ser2P) were determined in samples from leaf primordia < 2mm in length (LP) and in mature fully elongated leaves (ML) of 16 day-old plants with 8WG16, H14 and H5 antibodies (Abcam) respectively.

Figure S4. Nuclear accumulation of IYO-GFP correlates with cell differentiation (Related to Figure 6). GFP fluorescence pattern in *35S::IYO-GFP* and *35S::RPB10-GFP* plants at different stages of lateral root development. Arrows: cells accumulating nuclear IYO-GFP at the proximal end of the RAM; arrowheads: accumulation of nuclear IYO-GFP at the distal end of the RAM in root cap cells. Bar: 50 μm.

Gene name	Symbol	AGI code	$\log_2$ Wt/iyo	p-value
AGAMOUS	*AG*	At4g18960	0.82	0.00000479
APETALA3	*AP3*	At3g54340	0.67	0.00001521
SEPALLATA1	*SEP1*	At5g15800	0.55	0.00129990
SEPALLATA2	*SEP2*	At3g02310	0.47	0.00095834
SEPALLATA3	*SEP3*	At1g24260	0.56	0.00013556
PISTILLATA	*PI*	At5g20240	0.77	0.00034612
SEEDSTICK	*STK*	At4g09960	1.07	0.00001899
SHATTERPROOF1	*SHP1*	At3g58780	0.54	0.00113444
SHATTERPROOF2	*SHP2*	At2g42830	0.71	0.00015082
SPOROCYTELESS	*SPL*	At4g27330	0.30	0.00591017
APETALA2	*AP2*	At4g36920	0.47	0.00015887
APETALA1	*AP1*	At1g69120	0.04	0.80576105
LEAFY	*LFY*	At5g61850	-0.19	0.02608562
CAULIFLOWER	*CAL*	At1g26310	-0.01	0.92920803
UNUSUAL FLORAL ORGANS	*UFO*	At1g30950	-0.25	0.00911935
SHOOTMERISTEMLESS	*STM*	At1g62360	-0.38	0.02284795
KNOTTED-LIKE 1	*KNAT1*	At4g08150	-0.36	0.00209664
KNOTTED-LIKE 6	*KNAT6*	At1g23380	-0.27	0.00547389

Table S1. *IYO* is required for expression of developmental regulators in shoot inflorescence apices (Related to Figure 1). The mRNA profiles from 22 day-old Wt and *iyo-1* inflorescence apices were compared by microarray hybridization. The $\log_2$ of the ratio between the signals in Wt and *iyo-1* samples (mean of three biological replicates, each a pool of apices collected from 3 independent experiments) and the p-values from unpaired Student t-tests comparing those signals are presented. The homeotic flower organ identity genes *AG*, *AP3*, *SEP1*, *SEP2*, *SEP3*, *PI*, *AP2*, *STK*, *SHP1* and *SHP2* require *IYO* for proper activation. *LFY*, *AP1*, *CAL* and *UFO*, which promote inflorescence identity of the SAM, are expressed similarly and even at slightly higher levels in *iyo-1* apices, serving as internal controls that demonstrate that the *iyo-1* and Wt apices had both made the transition to flowering.

Supplemental experimental Procedures

Materials

The *iyo-1* mutant was isolated from an EMS-mutagenized population in the Landsberg *erecta* (Ler) ecotype. The *clv3-2*, *stm-6*, *elo2-1*, *elo3-1* and *elo4-1* (*drl1-4*) mutants are also in the Ler background. For all experiments involving mutants, Ler was used as the Wt control. In the crosses with marker lines (which were in the Col-0 ecotype) we compared *iyo-1* mutants with Wt siblings coming from the same crosses. We did not observe any effect of the mixed Ler/Col-0 constitution on the expression pattern of the markers. Transgenic lines were generated in the Col-0 ecotype that was used as Wt control. The *IYO* and *RPB3* (At2g15430) cDNAs were obtained from the ABRC. *RPB10* (At1g61700) was PCR amplified and cloned in pDONR vectors for GATEWAY recombination-based subcloning (Invitrogen). For bimolecular fluorescence complementation *IYO*, *RPB3* and *RPB10* were cloned in pBIF vectors and agroinfiltrated into leaves of *Nicotiana benthamiana* as described [2]. For expression of GFP and HA tagged fusions, cDNAs were cloned into pGWB vectors.

Microscopy analyses

Tissues were fixed and processed for *in situ* hybridization or scanning electron microscopy as previously described [3]. For histological analyses, shoot apices were similarly fixed and embedded in HistoResin, cut into 3 μm thick sections and stained with cresyl violet. For Nomarski microscopy, tissues were cleared in a solution containing an 8:3:1 mixture of chloral hydrate:water:glycerol and imaged with a Zeiss Axioskop microscope. For confocal microscopy plants were monitored using a Leica TCS SP5 laser scanning confocal microscope with propidium iodide as counterstain.

Microarray analysis

Total RNA from shoot apices was extracted using Trizol (Invitrogen) and microarray profiles were obtained as described [2]. Microarray data have been deposited at MIAMEXPRESS (*iyo-1* versus Wt inflorescence shoot apices: E-MEXP-1735).

In vitro pull-down assays

IYO and *iyo-1* (G962D allele) were cloned into pDEST-TH1 to obtain N-terminal MBP-fusions. Recombinant proteins were expressed in *Escherichia coli* and purified according to standard protocols. *In vitro* synthesis of RPB3 and ELO3 was done using a plasmid template with the TNT Coupled Wheat Germ Extract System (Promega) in the presence of [35S] methionine. Pull-down was performed as previously described [2].

RPB1 Ubiquitination

Seven-day old seedlings grown in liquid MS were treated for 6 h with 20 μM MG132 or and equivalent amount of solvent (DMSO), and homogenized in 50 mM Tris-HCl (pH 7.5), 150 mM NaCl, 1% SDS, 1% NP-40, 0.5% sodium deoxycholate, 10 mM N-ethylmaleimide and protease inhibitors (Roche). The homogenates were boiled for 10 min, centrifuged, and the supernatants used for immunoprecipitation by diluting in SDS-free extraction buffer to a final SDS concentration of 0.1%.

Supplemental references

1. Gendra E, Moreno A, Alba MM, Pages M. 2004. Interaction of the plant glycine-rich RNA-binding protein MA16 with a novel nucleolar DEAD box RNA helicase protein from Zea mays. Plant J 38, 875-886.

2. Chini, A., Fonseca, S., Fernandez, G., Adie, B., Chico, J.M., Lorenzo, O., Garcia-Casado, G., Lopez-Vidriero, I., Lozano, F.M., Ponce, M.R., Micol, J.L., and Solano, R. (2007). The JAZ family of repressors is the missing link in jasmonate signalling. Nature *448*, 666-671.
3. Aguilar-Martinez, J.A., Poza-Carrion, C., and Cubas, P. (2007). Arabidopsis BRANCHED1 acts as an integrator of branching signals within axillary buds. Plant Cell *19*, 458-472.